Structural determinants of the dictyostatin chemotype for tubulin binding affinity and antitumor activity against taxane- and epothilone-resistant cancer cells

Chiara Trigili[1], Isabel Barasoain[1*], Pedro A. Sánchez-Murcia[2], Katja Bargsten[3¤], Mariano Redondo-Horcajo[1], Aurora Nogales[4], Nicola M. Gardner[5], Arndt Meyer[5], Guy J. Naylor[5], Elena Gómez-Rubio[2], Federico Gago[2], Michel O. Steinmetz[3], Ian Paterson[5], Andrea E. Prota[3], and J. Fernando Díaz[1]*

[1]Chemical and Physical Biology, Centro de Investigaciones Biológicas, CSIC, Ramiro de Maeztu 9 E-28040 Madrid, Spain. [2]Área de Farmacología, Departamento de Ciencias Biomédicas, Universidad de Alcalá, Unidad Asociada al IQM (CSIC), E-28871 Alcalá de Henares, Madrid, Spain. [3]Department of Biology and Chemistry Laboratory of Biomolecular Research, Paul Scherrer Institut 5232 Villigen PSI, Switzerland. [4]Instituto de Estructura de la Materia, Consejo Superior de Investigaciones Científicas IEM-CSIC, Serrano 121, E-28006 Madrid, Spain. [5]University Chemical Laboratory, University of Cambridge, Cambridge CB2 1EW, United Kingdom.

*KB current address: Department of Biochemistry, University of Zurich, Zürich, Switzerland.

[¤]Corresponding author and lead contact: J. Fernando Díaz e-mail: fer@cib.csic.es; corresponding author for cell biology: Isabel Barasoain e-mail: i.barasoain@cib.csic.es

Content of supplementary information

Supplementary results

Simulation of epothilone A binding to a reduced representation of a MT.

The pharmacophore region accounting for the high-affinity binding of epothilone A to the taxane-binding site in a MT was revealed in atomic detail when the crystal structure of a stathmin/TTL-stabilized longitudinal assembly of two α,β-tubulin dimers in complex with one molecule of epothilone A was solved (PDB id. 4I50)[1]. An identical binding mode for epothilone A was subsequently reported in the ternary complexes of the same macromolecular assembly with two bound molecules of epothilone A and either laulimalide or peloruside A (PDB ids. 4O4I and 4O4L, respectively) concurrently bound in a non-taxane site[2]. Further insight into the structural determinants for binding was obtained when a simplified α,β-tubulin:epothilone A complex was simulated using MD, and models for other complexes with a series of epothilone A analogues were built to derive quantitative structure-activity relationships[3]. This earlier work revealed that the macrocyclic ring of epothilone A is engaged in hydrogen-bonding interactions with OD1/OD2(Asp226), N(Thr276), and NE2(Gln282), whereas the thiazole N22 of its side chain establishes an additional and rather unique hydrogen bond with OG1(Thr276). In addition, it was proposed that a water molecule bridging a hydrogen bond between the main-chain CO and NH groups of Leu217 and Arg278, respectively, could provide an extra anchoring point to the carbonyl oxygen at C5 of epothilone A (Figure S4)[3].

All of these hydrogen-bonding interactions were found to be present in sites 1 and 2 of our initial [epothilone A:(α1-β1-α2)]2 model but they evolved differently over the time course of the simulation. The one fluctuating most was

that involving the side-chain hydroxyl of Thr276, which appears to depend on a Thr276–Arg284–Glu290–Gln294 hydrogen-bonding network. The integrity of this network varies subtly in the different crystal structures and is heavily compromised in the absence of the canonical lateral contacts with the neighboring protofilament (site 1 vs. site 2). In contrast, the hydrogen bonds involving OD1/OD2(Asp226), N(Thr276), NE2(Gln281) and the water molecule bridging O(Leu217) and N(Arg278) are long-lived and show no significant differences between the two sites (Figure S4). This is of interest because adoption of an α-helical conformation by the segment Arg278–Tyr283 (the M-loop) of β-tubulin in crystals has been observed only in the presence of bound epothilone A, either alone[1] or in co-crystals with laulimalide or peloruside A[2]. In the complexes with these latter ligands alone[2] or in the complex with paclitaxel[4], this region appears disordered but is helical in the MTs studied by cryo-electron microscopy[5].

Analysis of the MD trajectories over ≥100 ns revealed that both epothilone A molecules are tightly bound by virtue of van der Waals and electrostatic interactions (Figure S4), including the contribution from the highly directional hydrogen bonds described above. It was also apparent that both the longitudinal and lateral contacts in tubulin, i.e. within and between the two protofilaments, were mostly maintained. After ~60 ns, however, it was noted that some of the ligand-protein and protein-protein hydrogen bonds in the neighborhood of the M-loop were lost in competition with water molecules, ions and/or exchange with other partners. As a consequence, although the M-loop kept its α-helical structure to a large extent and the OH(Tyr283) maintained the interaction with O(Glu85) in the neighboring β1' subunit, the side chains of

Gln281 and Arg284 extended away from the bound ligand and the side chain of Thr276. Taken together, our MD simulation results for the tubulin-epothilone A complex in the context of a MT are fully consistent with the experimental observations for a T2R-TTL-epothilone A complex, providing complementary theoretical insight into the dynamics of the interprotofilament region near the taxane-binding site. In fact, the differences observed between sites 1 and 2 can be taken as a reflection of the finding that MSA have more affinity for MT compared to tubulin dimers. Furthermore, these results also raise awareness of the previously recognized intrinsic limitations of using tubulin dimers as MT surrogates in MD simulations for computational tractability[6].

Supplementary Experimental Methods.

In silico model building and molecular simulations

This macromolecular ensemble was built as follows: (1) α-subunits A, E, I, K and β-subunits B and F were selected from the cryo-electron microscopy reconstructions (PDB code 3J6G) of kinesin-decorated MTs in complex with paclitaxel solved at ~5-Å resolution[5]; (2) missing residues 39-48 in the four α-subunits, together with the partially hydrated Ca^{2+} ion coordinated by Asp39, Thr41, Gly44, and Glu55 were "grafted" from α-subunit C of the 2.3-Å resolution structure (PDB code 4I50) of dimeric α,β-tubulin in complex with epothilone A (EpoA)[1] following a best-fit root-mean-square superimposition on the rest of the protein; (3) the M-loop (residues 274–287) and the Arg369-Leu371 loop in β subunits B and F adopted the conformation found in subunit D of PDB entry 4I50; (4) the two guanosine diphosphate (GDP) and four guanosine

triphosphate (GTP) molecules were preserved from the original 3J6G but the protein side chains in the nucleotide-binding site were slightly reoriented so as to make them establish equivalent interactions to those observed in the higher resolution PDB entry 4I50[1]; and (5) the docked poses of epothilone A and dictyostatin within the taxane-binding site (upon removal of paclitaxel) were those found in chain D of their respective crystallographic complexes with two α,β-tubulin dimers. In the complex with dictyostatin, an alternative rotamer from the built-in PyMOL library was chosen for Gln282 to prevent steric clashes and allow a better accommodation of the ligand.

The charge distributions for all the ligands studied were obtained by fitting the quantum mechanically calculated (HF/6-31G*//HF/6-31G*) molecular electrostatic potential (MEP), as implemented in Gaussian 09[7], to a restrained electrostatic potential (RESP) point-charge model[8]. The AMBER (http://ambermd.org/) force field leaprc.ff14SB was used to assign bonded and nonbonded parameters (parm14) to all ligand atoms. Conformational sampling for the ligands dictyostatin, **2**, **10**, and **11** was achieved after immersing each modeled molecule in a cubic box of ~1650 TIP3P water molecules[9] and running unrestrained MD simulations at 300 K for 100 ns.

The addition of missing hydrogen atoms to the protein ensemble and computation of the protonation state of titratable groups at pH 6.5 were carried out using the H++ 3.0 Web server[10]. Each complex was immersed in a cubic box containing ~108300 TIP3P water molecules plus 104 Na^+ ions to achieve electroneutrality and was simulated under periodic boundary conditions for 100 ns at 300 K. Electrostatic interactions were treated using the smooth particle mesh Ewald method[11] with a grid spacing of 1 Å. The cutoff distance for the

non-bonded interactions was 10 Å and the SHAKE algorithm[12] was applied to all bonds involving hydrogens. An integration step of 2.0 fs was used throughout. Subsequent gradual cooling followed by energy minimization provided representative structures for the complexes. Analysis of the MD trajectories was performed using the *cpptraj* routines implemented in AmberTools14[13] and our in-house MM-ISMSA software[14].

References

1. Prota, A. E.; Bargsten, K.; Zurwerra, D.; Field, J. J.; Diaz, J. F.; Altmann, K. H.; Steinmetz, M. O., Molecular mechanism of action of microtubule-stabilizing anticancer agents. *Science* **2013,** *339* (6119), 587-90.
2. Prota, A. E.; Bargsten, K.; Northcote, P. T.; Marsh, M.; Altmann, K. H.; Miller, J. H.; Diaz, J. F.; Steinmetz, M. O., Structural basis of microtubule stabilization by laulimalide and peloruside A. *Angew Chem Int Ed Engl* **2014,** *53* (6), 1621-5.
3. Canales, A.; Nieto, L.; Rodriguez-Salarichs, J.; Sanchez-Murcia, P. A.; Coderch, C.; Cortes-Cabrera, A.; Paterson, I.; Carlomagno, T.; Gago, F.; Andreu, J. M.; Altmann, K. H.; Jimenez-Barbero, J.; Diaz, J. F., Molecular recognition of epothilones by microtubules and tubulin dimers revealed by biochemical and NMR approaches. *ACS Chem Biol* **2014,** *9* (4), 1033-43.
4. Lowe, J.; Li, H.; Downing, K. H.; Nogales, E., Refined structure of alpha beta-tubulin at 3.5 Å resolution. *J. Mol. Biol.* **2001,** *313* (5), 1045-57.
5. Alushin, Gregory M.; Lander, Gabriel C.; Kellogg, Elizabeth H.; Zhang, R.; Baker, D.; Nogales, E., High-Resolution Microtubule Structures Reveal the Structural Transitions in αβ-Tubulin upon GTP Hydrolysis. *Cell* **2014,** *157* (5), 1117-1129.
6. Coderch, C.; Klett, J.; Morreale, A.; Diaz, J. F.; Gago, F., Comparative Binding Energy (COMBINE) Analysis Supports a Proposal for the Binding Mode of Epothilones to beta-Tubulin. *Chemmedchem* **2012,** *7* (5), 836-43.
7. Frisch, M. J.; Trucks, G. W.; Schlegel, H. B.; Scuseria, G. E.; Robb, M. A.; Cheeseman, J. R.; Scalmani, G.; Barone, V.; Mennucci, B.; Petersson, G. A.; Nakatsuji, H.; Caricato, M.; Li, X.; Hratchian, H. P.; Izmaylov, A. F.; Bloino, J.; Zheng, G.; Sonnenberg, J. L.; Hada, M.; Ehara, M.; Toyota, K.; Fukuda, R.; Hasegawa, J.; Ishida, M.; Nakajima, T.; Honda, Y.; Kitao, O.; Nakai, H.; Vreven, T.; Montgomery Jr., J. A.; Peralta, J. E.; Ogliaro, F.; Bearpark, M. J.; Heyd, J.; Brothers, E. N.; Kudin, K. N.; Staroverov, V. N.; Kobayashi, R.; Normand, J.; Raghavachari, K.; Rendell, A. P.; Burant, J. C.; Iyengar, S. S.; Tomasi, J.; Cossi, M.; Rega, N.; Millam, N. J.; Klene, M.; Knox, J. E.; Cross, J. B.; Bakken, V.; Adamo, C.; Jaramillo, J.; Gomperts, R.; Stratmann, R. E.; Yazyev, O.; Austin, A. J.; Cammi, R.; Pomelli, C.; Ochterski, J. W.; Martin, R. L.; Morokuma, K.; Zakrzewski, V. G.; Voth, G. A.; Salvador, P.; Dannenberg, J. J.; Dapprich, S.; Daniels, A. D.; Farkas, Ö.; Foresman, J. B.; Ortiz, J. V.; Cioslowski, J.; Fox, D. J. *Gaussian 09*, Gaussian, Inc.: Wallingford, CT, USA, 2009.
8. Vanquelef, E.; Simon, S.; Marquant, G.; Garcia, E.; Klimerak, G.; Delepine, J. C.; Cieplak, P.; Dupradeau, F. Y., R.E.D. Server: a web service for deriving RESP and ESP charges and building force field libraries for new molecules and molecular fragments. *Nucleic Acids Res.* **2011,** *39* (Web Server issue), W511-7.

9. Jorgensen, W. L.; Chandrasekhar, J.; Madura, J. D.; Impey, R. W.; Klein, M. L., Comparison of simple potential functions for simulating liquid water. *J. Chem. Phys.* **1983,** *79* (2), 926-935.
10. Anandakrishnan, R.; Aguilar, B.; Onufriev, A. V., H++ 3.0: automating pK prediction and the preparation of biomolecular structures for atomistic molecular modeling and simulations. *Nucleic Acids Res.* **2012,** *40* (Web Server issue), W537-41.
11. Cerutti, D. S.; Duke, R. E.; Darden, T. A.; Lybrand, T. P., Staggered Mesh Ewald: An extension of the Smooth Particle-Mesh Ewald method adding great versatility. *J Chem Theory Comput* **2009,** *5* (9), 2322.
12. Ryckaert, J.-P.; Ciccotti, G.; Berendsen, H. J. C., Numerical integration of the cartesian equations of motion of a system with constraints: molecular dynamics of n-alkanes. *Journal of Computational Physics* **1977,** *23* (3), 327-341.
13. Case, D. A. J. T. B., R.M. Betz, D.S. Cerutti, T.E. Cheatham, III, T.A. Darden, R.E. Duke, T.J. Giese, H. Gohlke, A.W. Goetz, N. Homeyer, S. Izadi, P. Janowski, J. Kaus, A. Kovalenko, T.S. Lee, S. LeGrand, P. Li, T. Luchko, R. Luo, B. Madej, K.M. Merz, G. Monard, P. Needham, H. Nguyen, H.T. Nguyen, I. Omelyan, A. Onufriev, D.R. Roe, A. Roitberg, R. Salomon-Ferrer, C.L. Simmerling, W. Smith, J. Swails, R.C. Walker, J. Wang, R.M. Wolf, X. Wu, D.M. York and P.A. Kollman *AMBER 2015*, San Francisco, 2015.
14. Klett, J.; Núñez-Salgado, A.; Dos Santos, H. G.; Cortés-Cabrera, Á.; Perona, A.; Gil-Redondo, R.; Abia, D.; Gago, F.; Morreale, A., MM-ISMSA: An Ultrafast and Accurate Scoring Function for Protein–Protein Docking. *Journal of Chemical Theory and Computation* **2012,** *8* (9), 3395-3408.
15. Karplus, P. A.; Diederichs, K., Linking crystallographic model and data quality. *Science* **2012,** *336* (6084), 1030-3.
16. Davis, I. W.; Murray, L. W.; Richardson, J. S.; Richardson, D. C., MOLPROBITY: structure validation and all-atom contact analysis for nucleic acids and their complexes. *Nucleic Acids Res.* **2004,** *32* (Web Server issue), W615-9.
17. Ho, S.; Sackett, D. L.; Leighton, J. L., A "Methyl Extension" Strategy for Polyketide Natural Product Linker Site Validation and Its Application to Dictyostatin. *J. Am. Chem. Soc.* **2015,** *137* (44), 14047-14050.

Supplementary Tables

Supplementary Table S1. Cytotoxicity of the compounds in ovarian cell lines both sensitive (1A9) and resistant to MSA (PTX10, PTX22 and A8) due to amino acid replacements in β-tubulin.

Compound	**1A9 (nM)**	**PTX10 (nM) F272V**	**R/S**	**PTX22 (nM) A366T**	**R/S**	**A8 (nM) T276I**	**R/S**
Paclitaxel	2.2 ± 0.7	81.4 ± 6	37	33 ± 2.0	15.0	3.7 ± 0.3	1.7
Dictyostatin	7.7 ± 0.2	8.5 ± 2.5	1.1	5.7 ± 1.8	0.7	1.5 ± 0.7	0.2
Discodermolide	1457 ± 182	1932 ± 201	1.3	2067 ± 592.5	1.4	1417 ± 142	1.0
3	40 ± 2	23.3 ± 2.1	0.6	51 ± 6.5	1.3	21 ± 1.4	0.5
4	8.7 ± 2.8	25 ± 3.6	2.9	13 ± 2.7	1.5	9.9 ± 0.4	1.1
5	6.8 ± 2	207 ± 54	30.5	21.2 ± 1.1	3.1	15.4 ± 2.2	2.3
6	25 ± 5	137 ± 12.35	5.4	80.4 ± 3.6	3.2	33.7 ± 2.8	1.0
7	7967 ± 338	>30000	>3	11050 ± 1333	1.4	8250 ± 328	1.0
8	25.5 ± 5.1	692 ± 4.8	27.2	42.5 ± 8.2	1.7	37.2 ± 1.9	1.4
9	5.4 ± 1.35	14.7 ± 1.7	2.7	8.1 ± 1.4	1.5	4.1 ± 0.3	0.7
10	26 ± 4.5	>5000	>200	38 ± 11	1.4	81 ± 5	3.1
11	18.2 ± 0.05	6687.5 ± 1010	368.4	78.5 ± 15.7	4.3	128.5 ± 5.2	7.1
12	1.2 ± 0.4	5.7 ± 1.4	4.7	3.3 ± 0.4	2.8	1.8 ± 0.2	1.5
13	51 ± 8.4	>5000	>98	166 ± 8.6	3.3	104 ± 3.4	2.0
14	125 ± 13	7537.5 ± 856.2	60.2	643 ± 48.4	5.1	143 ± 7.3	1.1
15	566 ± 105	>5000	>8	591.5 ± 84.4	1.0	314 ± 18.2	0.6
16	2583 ± 117	16167 ± 5068	6.2	4250 ± 50	1.6	4030 ± 541	1.6

Supplemental Table S2. Values calculated for the combination index (CI) between paclitaxel or peloruside A and the ligands studied.

Paclitaxel (nM) + dictyostatin (nM)	CI±Std Err.	*n*	P value
0.25+0.625	0.19±0.08	3	0.0108
0.5+1	1.48±0.2	3	0.1525
0.5+1.25	0.68±0.03	3	0.0099
0.5+1.875	0.67±0.2	3	0.1997

Paclitaxel (nM) + discodermolide (nM)	CI±Std Err.	*n*	P value
0.25+10	0.48±0.02	3	0.0015
0.5+10	0.37±0.01	3	<0.0001
0.5+20	0.64±0.01	2	0.017

Paclitaxel (nM) + 4 (nM)	CI±Std Err.	*n*	P value
0.5+1.4	0.26±0.02	3	0.0007
0.5+2.8	0.48±0.01	3	0.0004

Paclitaxel (nM) + 5 (nM)	CI±error est.	*n*	P value
0.25+1.375	0.2±0.01	3	0.0002
0.5+1.375	0.35±0.01	3	0.0002
0.25+2.75	0.61±0.03	3	0.0082
0.5+2.75	0.77±0.02	3	0.0099

Paclitaxel (nM) + 9 (nM)	CI±error est.	*n*	P value
0.5+2.475	0.54±0.02	3	0.0042

Paclitaxel (nM) + 10 (nM)	C±error est.	*n*	P value
0.5+22.5	1.3±0.01	3	0.0004

Paclitaxel (nM) +12 (nM)	CI±error est.	*n*	P value
0.25+1	0.40±0.003	3	<0.0001
0.5+1	0.36±0.2	2	0.0898

Peloruside A (nM) + dictyostatin (nM)	CI±std error	*n*	P value
4.5+0.625	0.59±0.07	3	0.0249
4.5+1.25	0.77±0.06	2	s.d.
9+1.25	1.4±0.3	3	0.4124
13+0.625	1.6±0.4	3	0.3824

Peloruside A (nM) + discodermolide (nM)	CI±std error	*n*	P value
4.5+7.5	0.44±0.1	4	0.0191
4.5+15	0.75±0.06	4	0.0274
9+15	1.2±0.15	3	0.4097
13+10	1.9±0.5	3	0.3228

Peloruside A (nM) + 5 (nM)	CI±std error	*n*	P value
4.5+1.375	0.68±0.1	4	0.0377
4.5+2.75	0.72±0.1	3	0.2716
9+1.375	1.15±0.35	3	0.7422
9+2.75	1.3±0.4	3	0.5635

Peloruside A (nM) + 12 (nM)	IC±error est.	*n*	P value
4.5+0.5	0.65±0.1	3	0.2578
9+0.5	1.3±0.3	3	0.5844
9+1	1.7±0.4	3	0.3228
13+0.5	1.9±0.6	3	0.3990

The P values were calculated using the *Student's t test* with the GraphPad Prism v4.0 software. *n* indicates the number of tests done. CI values with significant synergistic interactions are shown in red.

Supplementary Table S3. Average binding energy per residue (kJ mol^{-1}) of Dictyostatin and Epothilone A with β_1-tubulin, respectively, along the MD simulation of the [MSA:(α_1-β_1-α_2)]$_2$ complexes.*

Dictyostatin				Epothilone A			
site1 (β_1)		site2 ($\beta_{1'}$)		site1 (β_1)		site2 ($\beta_{1'}$)	
Residue	*Energy* ± s.d.	*Residue*	*Energy* ± s.d.	*Residue*	*Energy* ± s.d.	*Residue*	*Energy* ± s.d.
His229	-25.5±2.5	His229	-30.0±2.5	**Leu275**	-15.5±2.1	**Leu275**	-14.2±1.3
Arg278	-18.8±2.1	Arg278	-19.7±2.1	**Thr276**	-14.2±3.3	**Thr276**	-11.7±1.9
Asp226	-18.8±2.1	Asp226	-17.6±2.9	**Pro274**	-13.4±2.1	**Pro274**	-8.4±1.2
Leu217	-16.3±1.7	Leu217	-16.7±1.3				
Thr276	-15.9±1.7	**Thr276**	-15.9±1.7				
Leu371	-15.1±1.7	Leu371	-14.2±1.7				
Pro274	-13.0±1.3	**Pro274**	-12.6±1.3				
Leu230	-11.7±1.3	Leu230	-11.7±1.3				
Gln281	-9.6±1.7	Gln281	-9.2±2.1				

*Average per-residue interaction energies calculated in both [Dictyostatin:(α_1-β_1-α_2)]$_2$ and [Epothilone A:(α_1-β_1-α_2)]$_2$ complexes using MM-ISMSA[14] and 2000 frames from the MD simulations (30 ns → 50 ns). Only those energies > 8.4 kJ mol^{-1} are shown.

Supplementary Table S4. Data collection and refinement statistics.

	T2R-TTL-Dictyostatin
Data collection[a]	
Space group	$P2_12_12_1$
Cell dimensions	
a, b, c (Å)	104.0, 156.5, 179.1
Resolution (Å)	67.8 – 2.30 (2.36 – 2.30)
R_{meas} (%)	11.1 (424.7)
R_{pim} (%)	3.3 (121.2)
$CC_{1/2}$[b]	100.0 (26.2)
I/σI	18.7 (0.7)
Completeness (%)	99.8 (98.9)
Redundancy	13.4 (12.6)
Refinement	
Resolution (Å)	67.8 – 2.30
No. unique reflections	129857
R_{work}/R_{free} (%)	18.3 / 23.3
Average B-factors (Å^2)	
complex	82.2
Solvent	66.7
Ligands (chain B/D)	115.8 / 109.0
Wilson B-factor	59.9
Root mean square deviation from ideality	
Bond length (Å)	0.008
Bond angles (°)	0.928
Ramachandran statistics[c]	
Favored regions (%)	96.8
Allowed regions (%)	3.15
Outliers (%)	0.05

[a]Highest shell statistics are in parentheses. [b]$CC_{1/2}$= percentage of correlation between intensities from random half-datasets[15]. [c]As defined by MolProbity[16].

Supplementary Figures

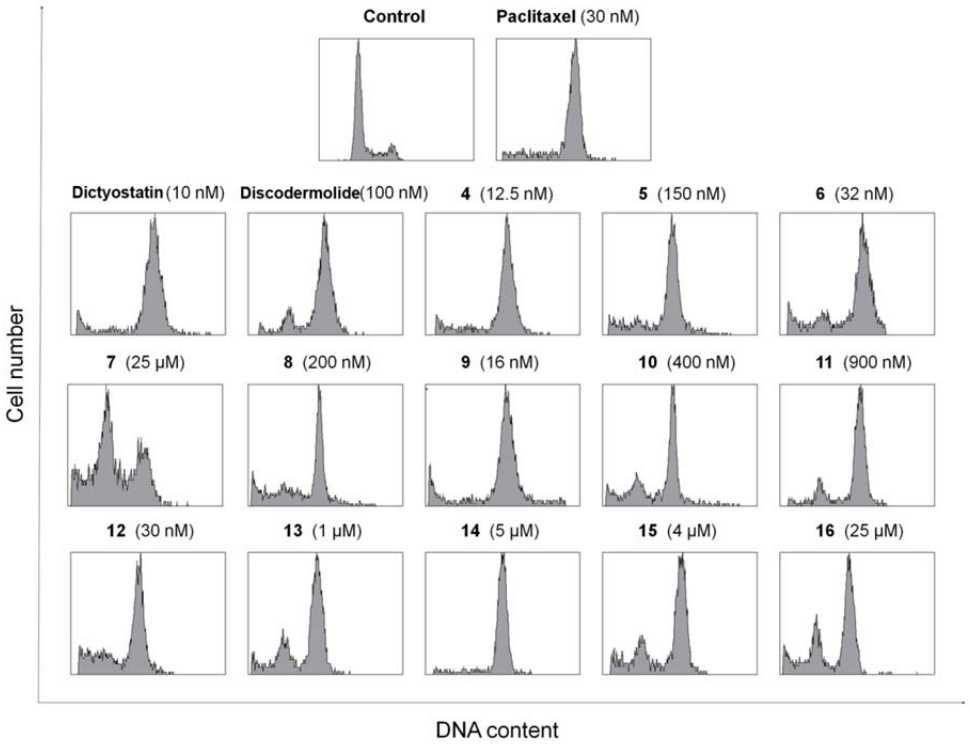

Figure S1.- **Effect of the ligands on the cell cycle of A2780 ovarian carcinoma cells.** Cells were treated for 19-20 h and labeled with propidium iodide. DNA contents were determined by cell cytometry.

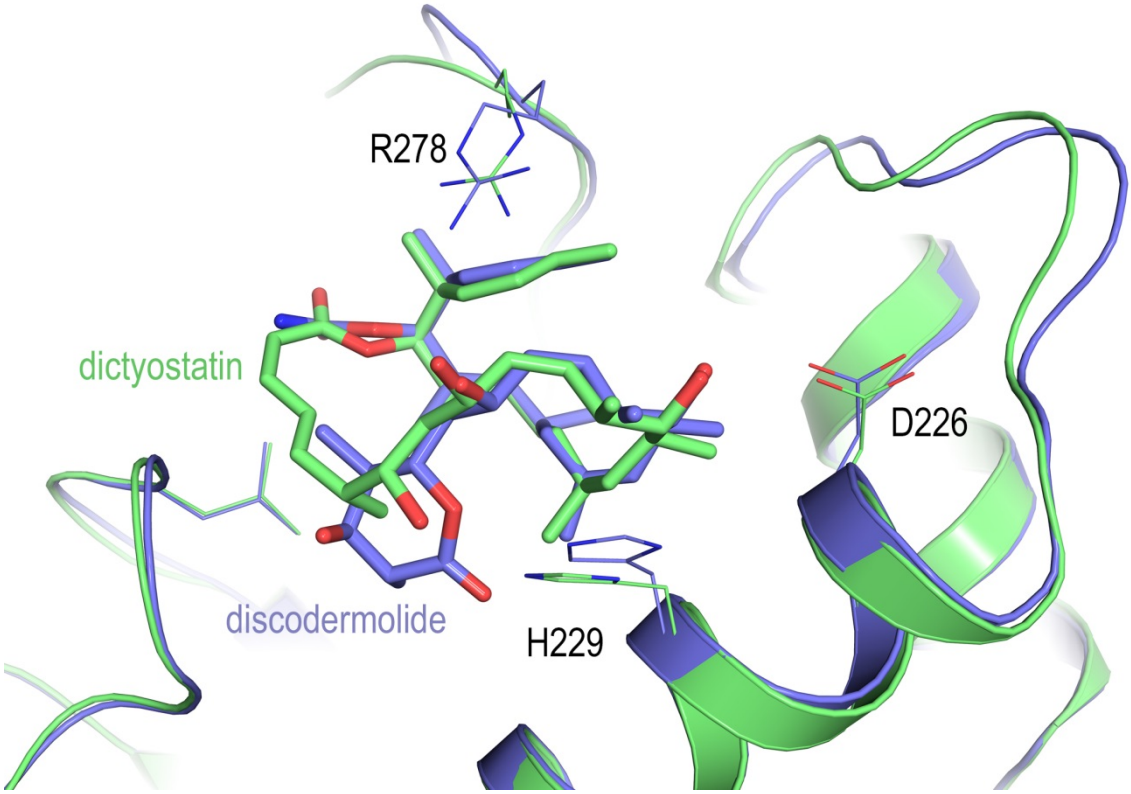

Figure S2.- **Comparison of the bound structures of dictyostatin and discodermolide**. Superposition of the binding sites on β-tubulin of both the complexes of T_2R-TTL-dictyostatin (green) and T_2R-TTL-discodermolide (slate) (Prota et al 2017 Submitted). Oxygen and nitrogen atoms are colored in red and blue, respectively.

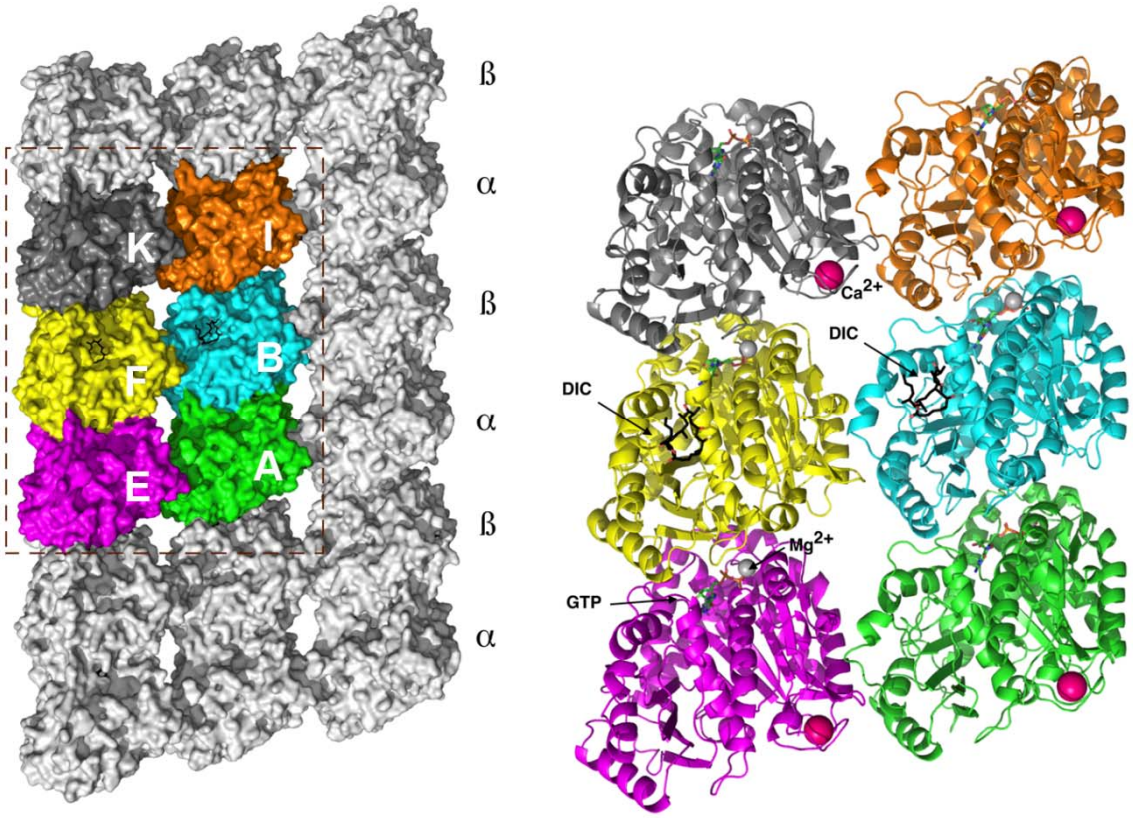

Figure S3. **Reduced representation of a microtubule used for the simulation**. (Left panel) Tubulin region selected from PDB structure 3J6G [5] and (Right panel) close-up view of the simulated microtubule segment (α-subunits A, E, I, and K and β-subunits B and F) in complex with a bound drug, DRG (either epothilone A or dictyostatin).

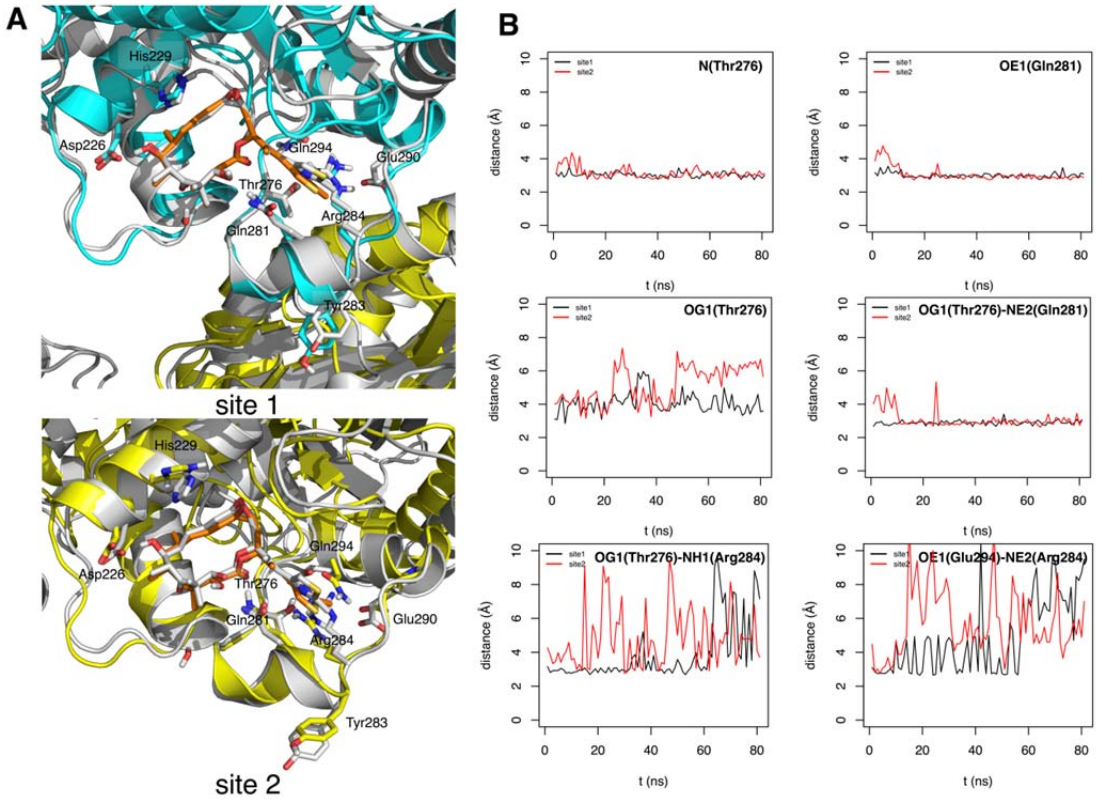

Figure S4. **Model of Epothilone bound to a microtubule.** (A) Superimposition of a representative structure of each major cluster of epothilone A conformers (C atoms colored in orange) bound to β-tubulin in subunit B (C atoms colored in blue, site 1) and F (C atoms colored in yellow, site 2) along the MD simulation (100 ns) onto subunit B of the X-ray crystal structure of dimeric tubulin in complex with epothilone A (C atoms colored in grey, PDB code 4I50). (B) Time evolution of distances (Å) relevant to the pharmacophore along the MD simulation in both B and F sites. (See also Figure S3)

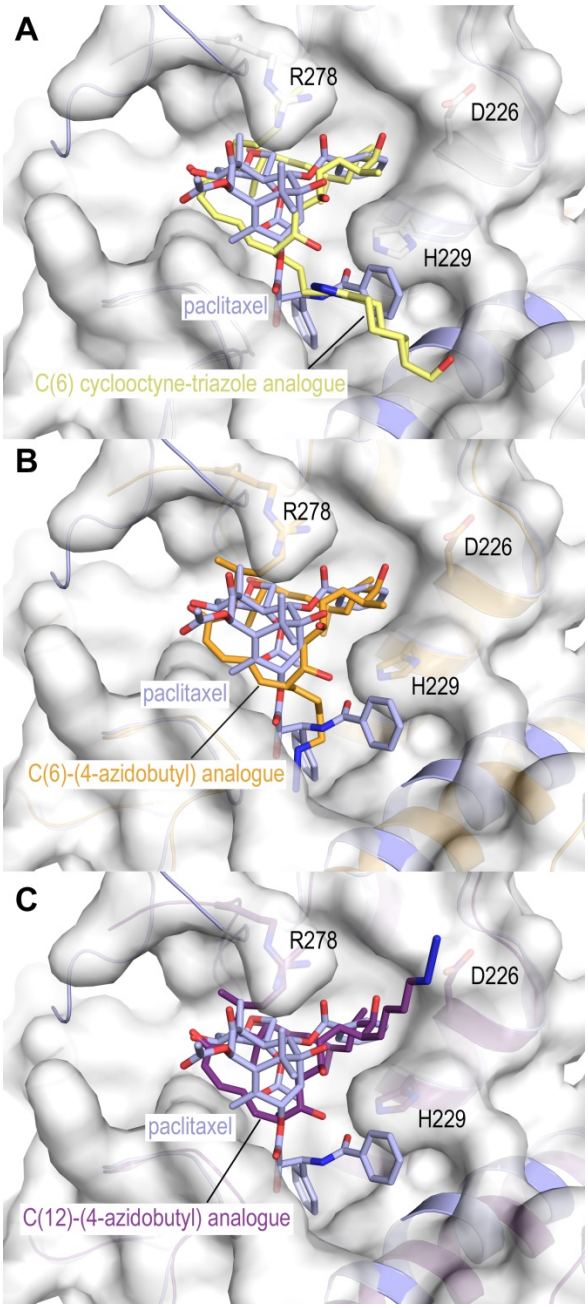

Figure S5.- **Modeled effect of substitutions at C6 and C12 in the ligand binding**. Panel (A) Superposition of the binding sites on β-tubulin of both the modeled C(6)-cyclooctyne-triazole dictyostatin analogue[17] and paclitaxel (PDB-ID 1JFF [4]). Carbon atoms are in yellow and light blue sticks, respectively. Panel (B) and (C) Superpositions of both the modeled C(6)- (orange) and C(12)-(4-azidobutyl) (violetpurple) analogues[17] onto the same as in (A). In all the panels, the β-tubulin chains of the corresponding complexes are in ribbon representation and are colored according to the same color code as the ligands. Moreover, to better highlight the taxane pocket, the β-tubulin chains of the dictyostatin-derivative complexes is displayed in transparent white surface representation.

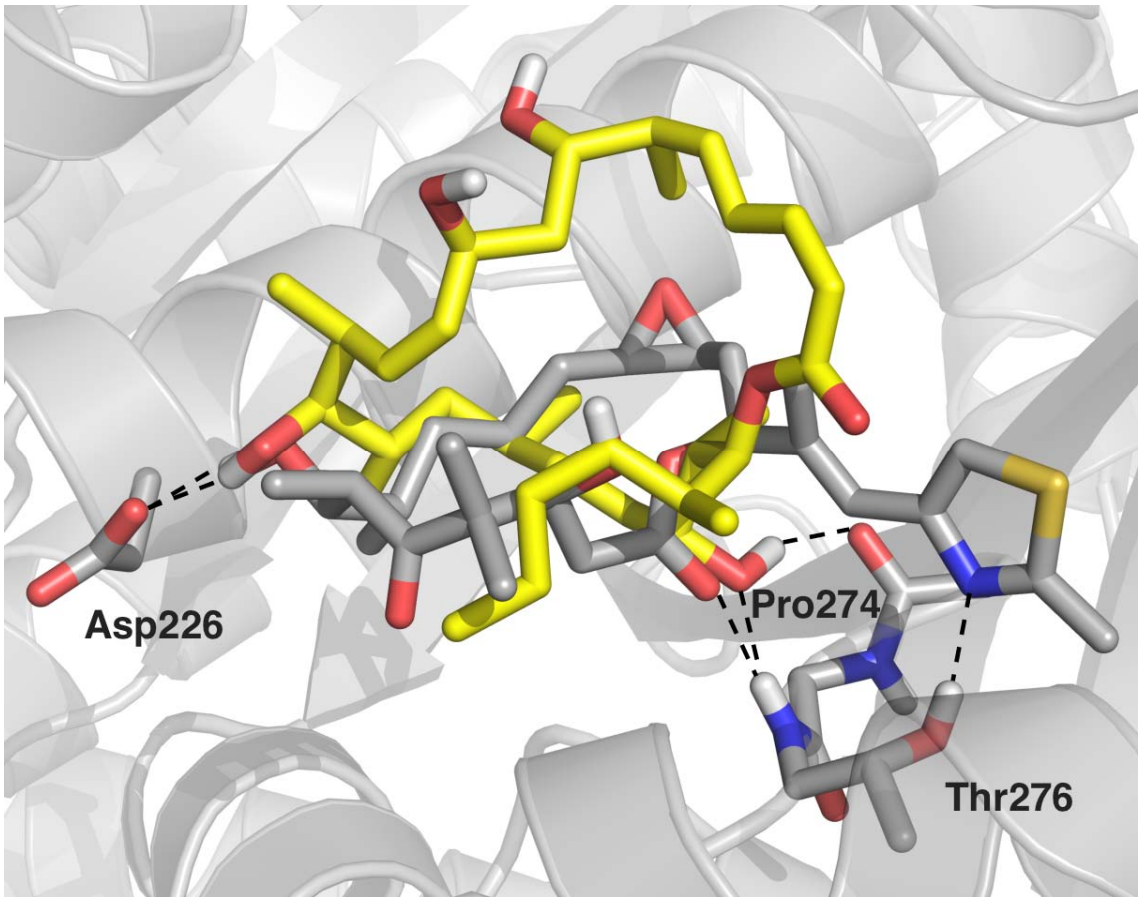

Figure S6.- **Superposition of the modelled binding modes of dictyostatin and epothilone A**. Best-fit superposition of the β_1 subunits of two representative [Epothilone A:(α_1-β_1-α_2)]$_2$ and [Dictyostatin:(α_1-β_1-α_2)]$_2$ complexes showing not only the common binding mode of dictyostatin and epothilone A (yellow and grey sticks, respectively). Residues providing hydrogen bonding donors and acceptors for both MSA are labeled.